Received July 6, 2019, accepted July 22, 2019, date of publication July 26, 2019, date of current version August 12, 2019.

Digital Object Identifier 10.1109/ACCESS.2019.2931311

Topological Transient Models of Three-Phase, Three-Legged Transformer

JIANHUI ZHAO[1], SERGEY E. ZIRKA[2], YURIY I. MOROZ[2], CESARE M. ARTURI[3], (Member, IEEE), REIGH A. WALLING[4], NASSER TLEIS[5], AND OLEXANDR L. TARCHUTKIN[6]

[1]College of Power and Energy Engineering, Harbin Engineering University, Harbin 150001, China
[2]Department of Physics and Technology, Dnipro National University, 49050 Dnipro, Ukraine
[3]Department of Electronics, Information and Bioengineering, Politecnico di Milano, 20133 Milan, Italy
[4]Walling Energy Systems Consulting, LLC, Clifton Park, NY 12065, USA
[5]Dubai Electricity and Water Authority, Dubai 564, United Arab Emirates
[6]Soft Team Group Ukraine, 69035 Zaporizhzhia, Ukraine

Corresponding author: Jianhui Zhao (zhaojianhui@hrbeu.edu.cn)

This work was supported in part by the National Natural Science Foundation of China under Grant 51879054, in part by the Postdoctoral Science Foundation of Heilongjiang Province of China under Grant LBH-Q18043, and in part by the Fundamental Research Funds for the Central Universities under Grant 3072019CF0305 and Grant 3072019CFG0301.

ABSTRACT The paper further develops a modeling concept of three-phase, three-legged transformer with tank walls represented as a distributed parameter structure. The circuital models proposed replicate accurately all possible zero-sequence impedances and losses of a three-winding transformer. Several model versions are compared to each other and to a conventional topological model with respect to their transient behavior during inrush and short circuit events, and in the presence of geomagnetically induced current (GIC). It was found that in all the cases considered, except that with a large GIC, all the models yield similar results. The reliability of the models is due to the representation of the tank walls behavior in a physical way, allowing one to observe the field distribution over the wall thickness as a function of transformer excitation. The modeled results are in a close agreement with positive and zero sequence data measured on a 25 MVA transformer as well as with inrush current test on a 300 kVA unit.

INDEX TERMS Tank influence, three-legged transformer, topological models, transients.

I. INTRODUCTION

Topological transformer models for low-frequency transients have been a subject of extensive studies over the last few decades. The state of art in this field was presented in [1] and, more recently, in [2] and [3]. Despite the obvious progress in their development, the topological models may still be inaccurate when the core approaches saturation [4]. This is primarily related to the commonly used three-legged core type transformers. As these transformers have no return limb to pass the zero-sequence (ZS) flux, the core saturation and different unbalanced conditions result in a significant off-core flux. An appreciable part of this flux penetrates into the transformer tank that makes the tank representation an important element of the whole transformer model.

Currently available tank models have been reviewed in [3] where no consensus was found among their authors. As far as we know, the only model demonstrated to accurately reproduce nonlinear nature of *all* ZS impedances of a three-legged transformer is that proposed in [5]. Although the model in [5] was extended to the transformer with vertical shunts [6], there are still unresolved issues in the tank representation. It was pointed in [3] that the tank model [5] needs to be tested for (i) zero-sequence power loss, (ii) global saturation of the tank under balanced over-excitation, for example in the presence of geomagnetically-induced current (GIC), and (iii) local saturation of the tank for unbalanced over-excitations, for instance during inrush current events or a single-phase to ground fault.

It should be noted that the above mentioned regimes are quite different in nature, and it is impossible to find a transformer tested in all these specific cases. Even confining the study to ZS characteristics, it is difficult to find transformer ZS impedances measured simultaneously with ZS power losses. To our knowledge, the only such study was reported in [7] and then by the same authors in [8] and [9]

The associate editor coordinating the review of this manuscript and approving it for publication was Bora Onat.

where linear steady-state transformer models have been proposed.

In such a situation, it is advisable to concentrate first on the model's ability to replicate all eight ZS characteristics of a 45/16.05/10 kV 25 MVA three-winding transformer provided in [7]. It will be shown that the ZS impedances and corresponding losses can be reproduced accurately using *different* sets of model parameters. So, having fitted the model using several parameter sets, we then examine their influence on the transformer behaviors during inrush current, single-phase to ground fault, and under GIC.

The models considered in Sections II to V can be classified as lumped-distributed circuits. In Section VI we also evaluate possibilities of the conventional topological model [10] in which ZS paths and associated losses are represented by per phase circuits L_0R_0.

II. TRANSFORMER MODELING IN ZS TEST

A simple experiment in which all magnetic flux leaves the core is the ZS test. In accordance with standards, the ZS impedance Z_0 is measured at the rated frequency between the line terminals of wye-connected windings connected together and their neutral. It is also noted in standards that the ZS impedance may have several values because it depends on how the other windings are connected. All possible ZS tests for a YNyn0d transformer are listed in Table 1 [7].

TABLE 1. Zero sequence test codes.

Test Code	HV winding	LV winding	Delta winding
HOO	Energized	Open	Open
HOC	Energized	Open	Closed
HSO	Energized	Short	Open
HSC	Energized	Short	Closed
LOO	Open	Energized	Open
LOC	Open	Energized	Closed
LSO	Short	Energized	Open
LSC	Short	Energized	Closed

The ZS impedances and the three-phase active power losses for the tests in Table 1 measured on the 25 MVA transformer in [7] are represented by separate dots in Figs. 1 and 2, respectively.

From the modeling perspective, the most challenging ZS tests are those designated as HOO and LOO in Table 1. The ZS *magnetizing* impedances measured in these tests are shown by upper points in Fig. 1.

In these tests, magnetic fluxes within the transformer tank are roughly sketched in Fig. 3 which depicts, for simplicity, only excited windings which are either high voltage (HV) or low voltage (LV) coils. All other windings are not shown in Fig. 3 because they are left open-circuited or unloaded.

A fundamental characteristic of the ZS test is that the ZS fluxes Φ_{0A}, Φ_{0B}, and Φ_{0C} in the legs are nearly equal in amplitude and phase, so there are no fluxes in the yokes. At the same time, the off-core paths of the ZS fluxes can be

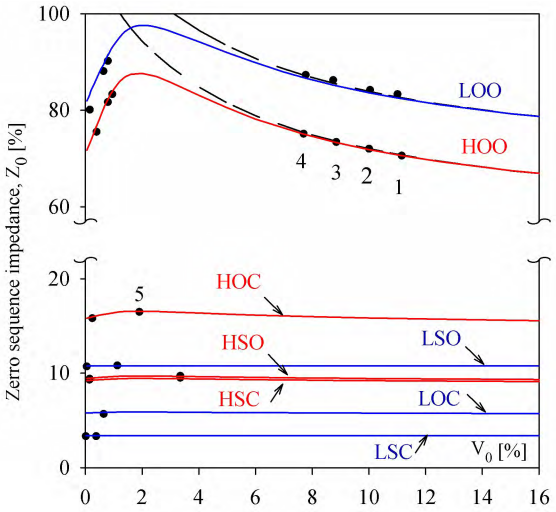

FIGURE 1. ZS transformer impedances measured in [7] (separate dots), and those calculated with the proposed transformer model (lines). Solid and dashed curves are for hysteresis and non-hysteresis tank representations, respectively.

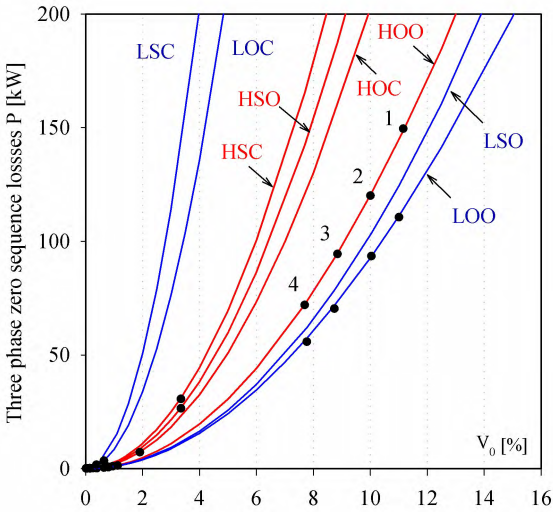

FIGURE 2. ZS power losses measured in [7] (dots) and those calculated with the transformer model proposed (lines).

quite different due to the asymmetrical position of the core in relation to all four tank walls.

This makes the transformer + tank arrangement a three-dimensional (3D) structure, which is quite complex and time-consuming to analyze with finite-element solvers [11].

To build a tractable *circuital* model, it is convenient to divide the off-core fluxes into the fluxes Φ_T entering the tank and the fluxes Φ_{YY} returning from yoke to yoke through non-magnetic paths between the tank walls and core legs. In turn, fluxes Φ_T can be subdivided into the fluxes Φ_{TC} entering the tank cover and those, Φ_{TW}, penetrating the walls. Somewhere in the upper part of the walls, fluxes Φ_{TC} and Φ_{TW} recombine into the flux Φ_T.

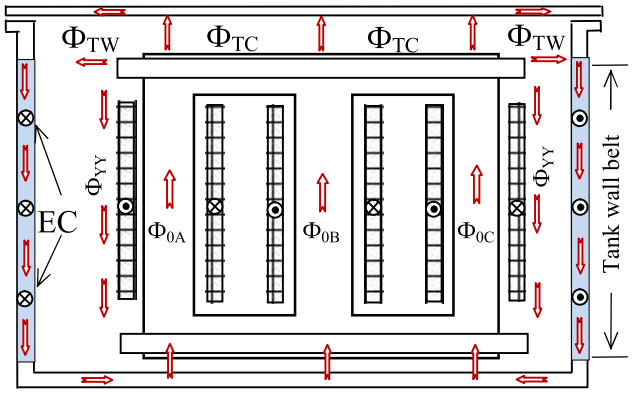

FIGURE 3. Magnetic fluxes and eddy currents in the tank walls of a three-legged transformer excited with the ZS single-phase voltage. The arrows show the reference directions of the alternative fluxes.

If the tank cover is farther from the core than the walls then it can be assumed, without the loss of generality, that no appreciable ZS flux enters the cover.

In the lower part of the walls, flux Φ_T passes to the tank bottom where it changes direction to find the shortest path to the lower core yokes.

The 3D nature of the transformer + tank arrangement in Fig. 3 is also caused by the fact that eddy currents, induced by the vertical time-varying flux Φ_T in the walls, flow horizontally, making the tank walls a closed single-turn winding, which encloses all three core legs and their windings [12], [13]. The outlined 3D flux pattern makes it difficult to evaluate ZS impedances and losses in acceptable time (the latter is important for transient modeling). Existing FEM solvers take hours or days to analyze even *quarter* transformer models [11], which are not suitable to simulate tank walls as a fictitious winding. Besides, as in the case of the transformer in [7], not all of its design parameters are often available.

In this situation, it is reasonable to develop further the simple transformer model proposed in [5]. The need for improving the model is caused by its 30 percent underestimate in predicting ZS power losses. This underestimate is due to the assumption that the ZS losses are only due to eddy currents (EC) designated in Fig. 3, which flow horizontally in the TWB along all four walls.

In the model described in Section III, we propose a simple means, which allows one to take into account the losses beyond the TWB. They may be caused by fluxes Φ_{TW}, which enter the walls normally or obliquely to their surface and induce eddy currents flowing *in the plane*of the walls. Besides, the losses in the tank bottom and cover are also accounted for indirectly in the updated electric model.

III. TOPOLOGICAL TRANSFORMER MODEL

The electric model of the three-winding transformer in Fig. 4 was obtained by applying the well-known duality transformation to the magnetic transformer model in Fig. 2 of [5]. The 1:1 turns ratio of three ideal transformers (ITs) at terminals of the middle winding 2 points out that the model parameters are referred to N_2 turns in this LV winding. Turn ratios n of ITs at terminals of the inner (delta-connected) winding 3 and the outer (HV) winding 1 are determined by corresponding voltage ratios.

In its main features, the model in Fig. 4 coincides with the model in Fig. 16 of [5], in which the processes in the legs and yokes are reproduced by DHM-inductors, which are ATP implementations of the dynamic hysteresis model (DHM) [14], [15].

If L_{S12}, L_{S23}, and L_{S13} are leakage inductances between windings 1-2, 2-3, and 1-3, respectively, then

$$L_p = (L_{S13} - L_{S12} - L_{S23})/2, \tag{1}$$

$L_{12} = L_{S12} + L_p$ and $L_{23} = L_{S23} + L_p$. The negative inductances in the vertical branches ($-L_p$) are to satisfy all three leakage inductances of the transformer [5].

The paths of the yoke-to-yoke flux Φ_{YY} are characterized by three linear inductances L_{YY}, and the paths of flux Φ_T are determined by three inductances L_T.

The TWB of the height h_T and thickness d is represented by a ladder Cauer circuit consisting of n pi-cells ($n = 15$ in Fig. 4). Each of the SHM-inductors characterizes a vertical flux tube with length h_T and cross section $p_T \times \delta$ where p_T is the tank perimeter and $\delta = d/n$ is the thickness of the tank wall "layer". When using EMTP-ATP, the SHM-inductors [16] can be employed. Eddy-current resistances R of the layers are calculated as $N_2^2 p_T \rho/(h_T \delta)$ where ρ is the resistivity of the tank steel. If necessary, resistances R can be made temperature-dependent, as suggested in [17].

It was found in numerical experiments that all ZS tests are reproduced accurately using the Cauer circuit with $n = 15$. When modeling other abnormal regimes, the circuit with $n = 25$ was found to be acceptable.

A simple but important improvement to the model is a tank loss resistor R_{loss}. Its *parallel* connection with the wall Cauer circuit in the duality-derived model of Fig. 4 means that in the parent *magnetic* model, this element is in *series* with the TWB. This means that R_{loss} allows one to cover the losses in the tank parts, which are above and below the TWB. These include tank bottom and cover, as well as the magnetic structural parts. As the detailed loss evaluation in these non-homogeneous elements is hardly possible within the electric model, the use of the *effective* R_{loss} is an appropriate method to reproduce unaccounted ZS losses. It is important that the value of R_{loss} meeting one of the ZS tests provides necessary increases in ZS losses in all the other ZS tests.

Before studying transformer behavior under overexcitation conditions, the model was fitted to measured no-load losses. When using the ATP model in Fig. 4, the fitting can be carried out by selecting a core material from the DHM library [15] and choosing its loss coefficient K_{loss} [14]. As seen in Fig. 5, the use of steel 27ZDKH85 provides sufficient approximation of the measured losses in the whole voltage range.

Fig. 5 also shows that at the voltages normally used in ZS tests, i.e. at V < 10-12%, the core losses can be neglected.

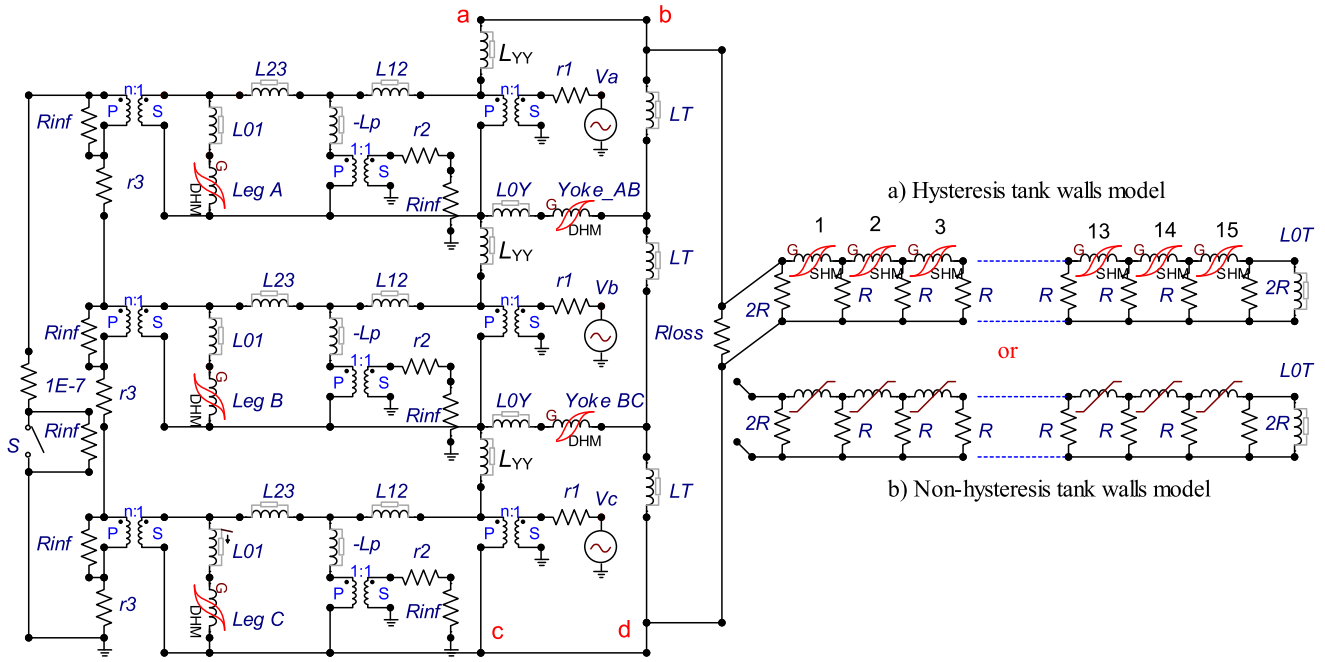

FIGURE 4. Electric model of the three-winding, core type transformer with (a) hysteresis or (b) non-hysteresis tank walls. Three-phase voltage source is on the HV side. Switch S opens the inner tertiary winding.

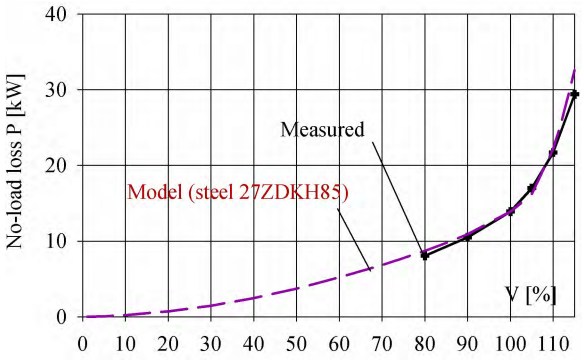

FIGURE 5. Positive sequence no-load power losses measured (solid line) and calculated (dashed line) with the model of the core type transformer.

This means that the ZS impedances are almost not sensitive to the core material.

IV. MODEL FITTING TO ZS TEST REPORT

Irrespective of the model version considered in this study, the model is always fitted so that the Z_0-curve HOO in Fig. 1 passes through points 1 to 4. This is achieved by varying only inductances L_{YY} and L_T. A useful observation is that increasing L_{YY} moves the Z_0 curve upward, whereas increasing L_T makes it steeper near the mentioned points 1−4. The per unit (pu) values of iteratively found inductances L_{YY} and L_T are listed in Table 2 where the ZS loss error is the average error in predicting the total transformer losses for the points 1 to 4.

TABLE 2. Model characteristics and parameters.

Model	TWB height / R_{loss} (Ω)	L_{YY} [pu]	L_T [pu]	ZS loss error [%]
M1	60% / No	0.3863	0.5945	-33.4
M2	95% / No	0.4528	0.6342	-30.8
M3	60% / 50	0.4162	0.8232	-1.8
M4	95% / 58	0.4817	1.3110	+0.1

The model 1 (M1) in Table 2 is the model in [5], in which the height of the TWB is equal to the height of the core window, as suggested in [18], or nearly 60% of the tank wall height as pointed out in the table. The ZS loss error (-33.4%) of model 1 points out that the losses in the TWB reproduce about 67% of the total ZS loss.

The model 2 (M2) in Table 2 illustrates the important fact that no substantial change in the ZS loss occurs if the height of the TWB is increased to the core height, becoming 95% of the wall height. As pointed out in Table 2, no resistor R_{loss} is used in models 1 and 2.

The models 3 (M3) and 4 (M4) in Table 2 contain R_{loss} and their TWB height is again equal either to 60% or 95% of the wall height, respectively.

For any given R_{loss}, a pair L_{YY} – L_T is found as described above in this Section, and the loss discrepancies at points 1 to 4 (in Fig. 2) are evaluated. So, starting at $R_{loss} = 0$, the value of this resistor is increased in steps until the loss values at points 1 to 4 are approximated accurately. Corresponding values of R_{loss}, L_{YY}, and L_T are given in Table 2.

After fitting the models to the values determined by points 1 – 4 in Figs. 1 and 2, the zero sequence impedances

and the corresponding losses were checked against all other measured values without any further fitting of the model. The fairly accurate prediction of transformer behavior at any other voltage and winding connection confirms the underlying physics of the model. In particular, the model with hysteretic steel of the tank reproduces the peaked curves HOO and LOO in Fig. 1 and even a subtle peak in curve HOC near point 5.

It should be pointed out that all these peaks disappear if the modeling is carried out using a *middle* (anhysteretic) curve of the tank material. In this case, the hysteretic inductors SHM in the model of Fig. 4(a) are replaced by nonlinear inductances shown in Fig. 4(b). It is shown in Fig. 1 that at low voltages, the dashed curves LOO and HOO, calculated with such an anhysteretic model, deviate from the corresponding solid curves. At the same time, the ZS losses provided by anhysteretic models are only some three percent less than those predicted by the models with "hysteretic tank". This is in accordance with the estimation in [19] that "hysteresis losses tend to be small relative to eddy current losses in the tank". It was also recently shown in [17] that dynamic losses dominate over hysteresis losses at all induction levels and frequencies in 4- and 6-mm thick tank steels studied in [17].

This allows one to make practical calculations using the simple non-hysteretic tank model, whilst utilizing the hysteresis tank representation to illustrate the underlying physics of the model.

It should be said that the curves in Figs. 1 and 2 are calculated for model 4 of Table 2. However, the model 3 gives almost the same ZS characteristics. This means that from the viewpoint of the ZS behavior, the height of the TWB (with corresponding L_{YY}, L_T, and R_{loss}) is a free parameter of the model. This allows one to use the TWB height as an additional variable, which can control the model behavior in regimes different from those in ZS tests.

In concluding this section, it is useful to consider the commonly-used concept of the skin effect and its applicability to the tank walls during Z0 tests, for example in the test HOO. As the skin depth is evaluated through a constant permeability μ (the tank material is thus supposed to be magnetically linear), it is instructive to compare processes inside tank walls calculated for a hypothetical linear and the real (saturable) tank materials.

In the linear case, the straight *B-H* line of the tank steel can be aligned with the initial (linear) part of the middle curve of the steel. The calculations carried out with a linear Cauer circuit yield an unrealistically high induction (8 Tesla) at the inner wall surface (see Fig. 6) and near exponential decrease in the induction peaks along the tank wall thickness d.

Quite different flux density envelope (solid curve in Fig. 6) is obtained for the real tank steel in which the rise of the surface flux density in Fig. 7 is limited by the saturation. This compels the next wall layers to reach higher flux densities than those in the linear material.

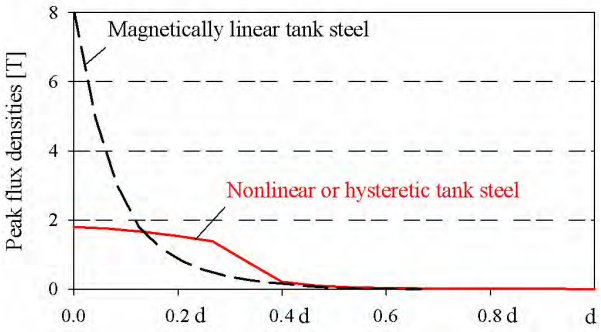

FIGURE 6. Envelopes of maximum flux densities over the wall thickness *d* calculated in the HOO test.

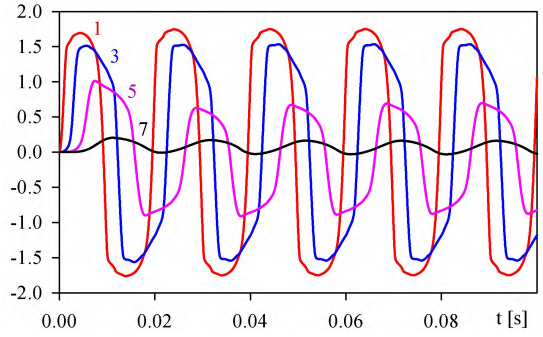

FIGURE 7. Flux densities in the 1, 3, 5, and 7 layers of the 15-layer tank wall during HOO test.

V. MODEL BEHAVIOR UNDER OVEREXITATION CONDITIONS

From a variety of possible cases in which the tank model is considered to be important, we confine ourselves to analysis of inrush currents, a single-phase to ground fault, and transformer behavior under GIC conditions. These regimes are chosen to show their qualitative and quantitative difference regarding the processes in the tank walls and different impacts of the tank representation on the modeled results.

In accordance with [7], the 45 kV HV network has 2500-MVA short-circuit (SC) power, and thus SC per phase impedance $Z_1 = 45^2/2500 = 0.81\ \Omega$. For the 45 kV network considered, resistance R_1 and reactance X_1 of impedance Z_1 can be deduced from the typical ratio $R_1/X_1 = 0.2$. So, in this Section, the network is represented by positive and zero sequence inductances 2.526 mH and resistances 0.162 Ω. For comparison, the leakage inductance between HV and LV transformer windings referred to the HV side is 27.74 mH.

To make transformer characterization more complete, inrush currents and one-phase ground faults on the yn side are modeled for the four winding connections listed in Table 3. Among them, the Yyn connection (the one with the ungrounded HV neutral and without delta) is not often used in practice, but was found to be most influenced by the tank representation. Each cell of Table 1 also contains a mean characteristic calculated with models 1 to 4 defined in Table 2. The bracketed percentages indicate maximum

TABLE 3. Inrush and SC currents found with models 1 to 4.

Winding connection	Model	Inrush current [A]	SC current peak [A]	SC current r.m.s. [A]
YNyn	M1	1449	7047	2743
	M2	1472	7069	2748
	M3	1404	7071	2746
	M4	1389	7073	2740
	Mean	1429	7065	2744
	(Max. dev.)	(3.0%)	(0.3%)	(0.2%)
YNynd	M1	1290	7225	2837
	M2	1318	7250	2846
	M3	1245	7252	2844
	M4	1235	7253	2839
	Mean	1272	7245	2842
	(Max. dev.)	(3.6%)	(0.3%)	(0.2%)
Yyn	M1	953	2693	881
	M2	954	2650	861
	M3	910	2669	868
	M4	876	2626	844
	Mean	923	2659	864
	(Max. dev.)	(5.1%)	(1.3%)	(2.3%)
Yynd	M1	1279	5548	2225
	M2	1307	5561	2230
	M3	1234	5558	2228
	M4	1224	5553	2221
	Mean	1261	5555	2226
	(Max. dev.)	(3.6%)	(0.15%)	(0.22%)

deviations of the values found with models 1 - 4 from the given means.

To explain the small difference between the models 1 to 4 (small deviations in Table 3), inrush current events and fault currents are considered in Sections V-A and V-B.

A. TANK BEHAVIOR DURING INRUSH CURRENT TRANSIENTS

When modeling inrush currents, we assume a demagnetized and unloaded transformer model in Fig. 4, which is connected to the voltage sources at the instant ($t = 0$) when the voltage of phase A crosses zero. The current waveforms in Fig. 8 are calculated with model 4 in Table 2, but similar processes are peculiar to all other models of the table, as can be seen in small percentages provided in the brackets of Table 3.

The largest is the current peak in phase A found for YNyn transformer, for which phase currents B and C are also depicted in Fig. 8. To avoid overloading the figure, only currents A are shown for YNynd and Yyn connections.

Fig. 9 shows flux densities in the legs of the YNyn transformer. The rounded peaks of the waveforms indicate leg saturation beyond ±2 T. (Recall that 2 T is the saturation induction of grain-oriented steels). The curve ZS in Fig. 9 is the sum of the shown flux densities, which can be recalculated into the ZS flux.

The shape of curve ZS in Fig. 9 is reflected in the shape of the flux density in the inner wall layer shown by the curve Inner (YNyn) in Fig. 10. As the ZS flux is comparatively small in the YNyn transformer, it does not reach the middle of the wall (the curve Middle (YNyn) looks like a horizontal line).

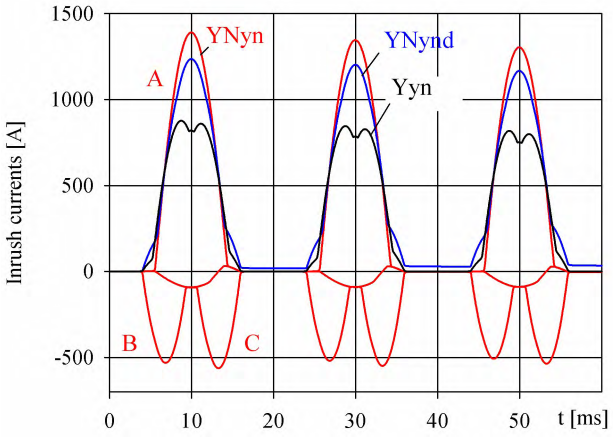

FIGURE 8. Inrush currents calculated on the HV terminals.

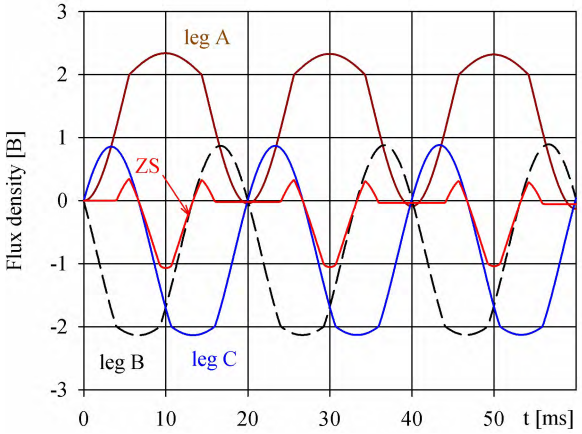

FIGURE 9. Flux densities in the legs of YNyn transformer and their sum (curve ZS).

It is noted in Fig. 8 that current peaks predicted at the closed delta winding, i.e. in the YNynd transformer, are some 10% less than those calculated in the YNyn unit. The fluxes in the tank become negligibly small in the presence of delta that makes YNynd transformer less informative from the viewpoint of the tank modeling. So, YNynd transformer is not considered in more detail in this Section.

Somewhat unusual, in Fig. 8, are smaller two-humped peaks calculated for Yyn transformer. Their shape and height (923 A in Table 3) can be explained by the floating neutral point N and the neutral-to-ground voltage oscillating within ±12 kV during the inrush transient.

In this case, there is a large flux density in the tank wall layers (see curves Yyn in Fig. 10) showing that the walls play the role of an external, closed delta winding. Model 1 was tested experimentally in [20] where the predicted inrush current peak on the HV side of a 300 kVA Yyn transformer was only 3% lower than the measured one.

The neutral shift is substantially decreased if the actual inner delta winding is closed. The fluxes in the walls of Yynd transformer are also decreased and inrush current peaks are

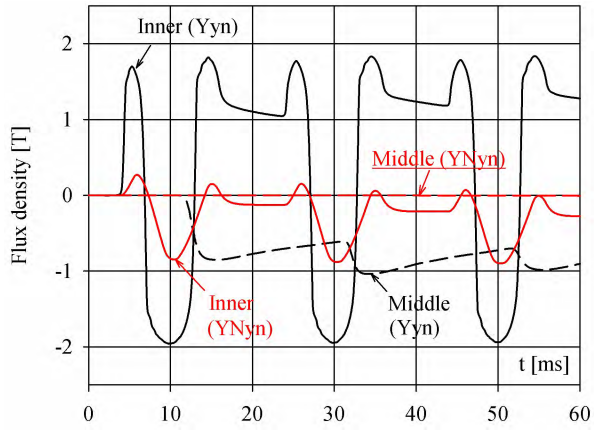

FIGURE 10. Flux densities in the inner and middle wall layers of the YNyn and Yyn transformers during inrush current transients.

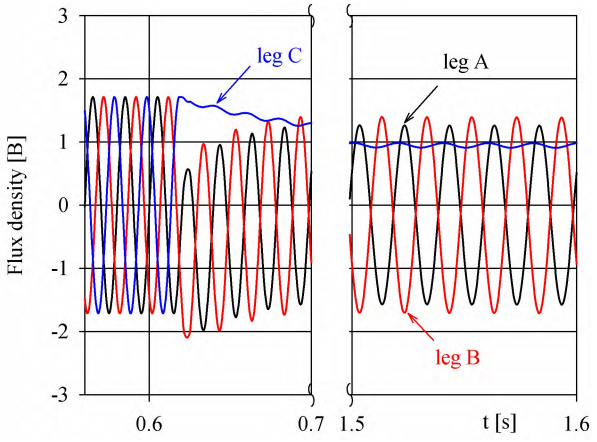

FIGURE 12. Flux densities in the legs of YNynd transformer during SC fault.

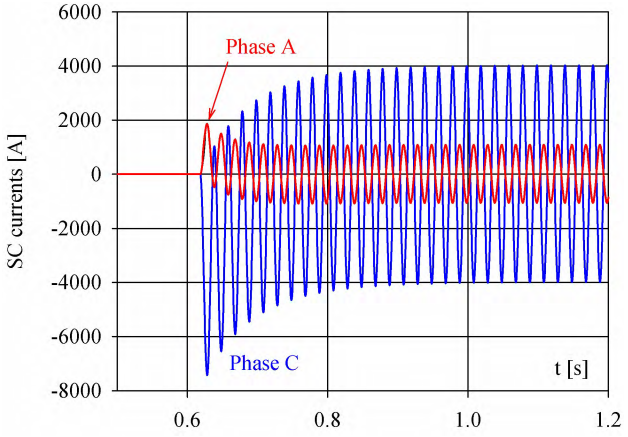

FIGURE 11. SC currents in YNynd transformer calculated with model 4.

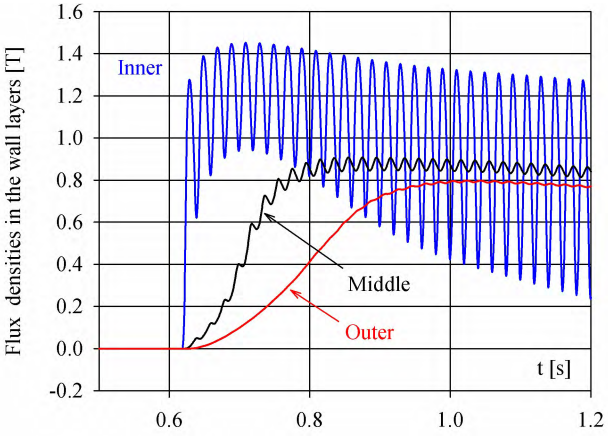

FIGURE 13. Flux densities in the tank wall layers of YNynd transformer during SC fault.

increased (1261 A in Table 3), making the current peak close to that (1272 A) calculated for YNynd connection.

B. TRANSFORMER MODELING AT SINGLE-PHASE FAULT

Because fault currents are typically much larger than load currents, it is assumed that there are no loads on the LV side when the transformer is supplied from the HV side. At the instant when C-phase voltage on the HV side crosses zero, the LV side phase C is solidly grounded.

As shown in the two last columns of Table 3, maximum fault current (in phase C on the HV side) was found, as expected, in YNynd transformer. Its waveform calculated with model 4 can be seen in Fig. 11, in which phase currents A and B practically coincide after the fault instant due to the balancing effect of, primarily, the actual, closed delta winding, as well as the tank walls that act as a virtual closed delta winding. Flux densities in the core legs and in the tank wall layers are shown in Figs. 12 and 13, respectively.

Detailed study of single-phase faults for different winding connections deserves a separate dedicated paper. The only conclusion to be drawn from the summary Table 3 is that SC fault currents calculated with models 1 to 4 for a given winding connection have very close peak and rms values in steady-state. (The deviations from the mean values never exceed 2.3 percent).

C. MODEL BEHAVIOR UNDER GIC CONDITIONS

To analyze the behavior of the transformer considered in the presence of GIC, it is supposed that a source of dc step voltage is introduced (at $t = 0.5$ s) between the HV neutral and the earth of the modeled circuit.

The transient and steady-state phase currents calculated for model 1 of Table 2 are similar to those in Figs. 10 and 11 of [3], which correspond to open and closed delta winding respectively. As in [3], the transients under GIC are predicted for the case when the dc voltage provides a 300 A dc current in the HV neutral (in steady state) and thus 100 A dc current in each of the phase windings.

The main indicator of transformer operation under GIC is the reactive power Q consumed from the network [21]. The values of Q predicted by models 1 to 4 are summarized

TABLE 4. Reactive power and maximum flux density in the legs.

	YNyn		YNynd	
Model	Q [Mvar]	B_m [T]	Q [Mvar]	B_m [T]
M1	0.386	2.0126	0.426	2.0157
M2	0.653	2.0188	0.719	2.0227
M3	1.007	2.0261	1.122	2.0311
M4	1.573	2.0377	1.762	2.0443
[10]	0.113	1.9987	0.126	2.0006

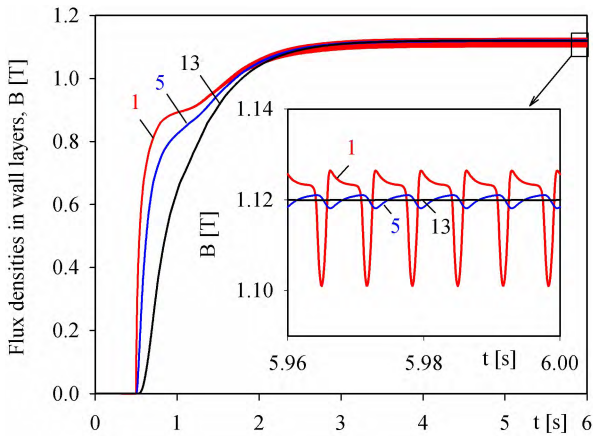

FIGURE 14. Flux densities in the 1, 5, and 13 layers of the 25-layer tank wall of YNyn transformer under GIC.

in Table 4, which also contains the Q value calculated with model [10] considered in Section VI.

The main thing to note in Table 4 is that different models with the same Z0 predict quite different reactive powers. This suggests that Z0 itself has no direct relation to transformer behavior under GIC. The reason may be in that the tank behavior during the ZS test employed for the model fitting is qualitatively different from that in the presence of GIC. This is because the ZS test is essentially a power frequency *ac* test, whereas the steady-state flux densities in all the tank wall layers under a large GIC seem almost constant on the scale of Fig. 14. (In the calculations with model 1, the wall thickness (8 mm) was divided into 25 layers).

Small oscillations seen in the magnified inset of Fig. 14 completely disappear in YNynd transformer.

Models 3 and 4, which provide realistic ZS losses due to the introduced resistor R_{loss}, predict much higher reactive powers (1.007 and 1.573 Mvar) than models 1 and 2 (with Q = 0.386 and 0.653 Mvar), which have the same TWB heights.

It is remarkable, however, that no changes occur in the results predicted by models 3 and 4 (in the presence of GIC) if resistor R_{loss} is omitted from these models, with other parameters kept unchanged. This is in accordance with eddy-current nature of R_{loss} and the fact that all eddy-currents disappear under almost *dc* conditions taking place in the tank at large GIC.

As models 1 and 2 differ in the height of the TWB, this value, as suggested above, can be used as a model variable. This conclusion is supported by the fact that inductance $L_{0\text{T}}$ (it characterizes the space beyond the tank) has no visible influence on the model behavior under GIC considered.

Although no GIC test was carried out on this particular transformer that could be used to verify the differences in its reactive power consumption as predicted by models 1-4 (they are listed in Table 4), it can be recalled that the GIC influence is not a critical issue for three-legged (3L) transformers. This is because 3L transformers are far less sensitive to GIC than *analogous* five-legged (5L) counterparts.

To demonstrate this fact, starting from the model considered, we should insert the DHM inductors into conductors *a-b* and *c-d* of the circuit in Fig. 4 to reproduce the end limbs of 5L transformer. The transformer's wound legs and windings are kept equal to those in the 3L unit, but the cross sections of the yokes and the end limbs are taken equal to 60 and 50 percent of the main leg area. The core geometry is completed by assuming the widths of the lateral windows equal to half the main window width. Our calculations carried out with thus obtained 5L model predict some 20 times greater reactive power consumption and twice less flux in the tank compared to those in the 3L transformer.

VI. TRANSFORMER MODEL WITH LUMPED ELEMENTS

From a practical viewpoint, it is desirable to use a simple transformer model capable of simulating zero sequence impedances and losses. A useful topological model, in this regard, is the one described in [10], which should be extended to a three-winding transformer and supplemented by inductances L_{01} lost in [10] when passing from the magnetic circuit in Fig. 11(b) to its electric equivalent in Fig. 11(c). Such a model can be obtained by short-circuiting inductances L_{T} in Fig. 4 and shunting inductances L_{YY} (inductances L_0 in [10]) by suitable resistances R_0.

This cuts off the Cauer circuit and reduces the model in Fig. 4 to the form shown in Fig. 15. The thus obtained L_0R_0 model is a compact equivalent of the model [10] in which L_0 and R_0 are split into two equal halves.

The values L_0 and R_0 of the model can be calculated with formulae in [10] or easily found iteratively by numerical simulations. It should be noted that the pair $L_0 - R_0$ depends on the measured Z_0 and P_0 to which the model is adjusted at a given V_0. The almost horizontal lines HOO and LOO in Fig. 16 illustrate the case when the model is fitted so as to meet ZS impedance ($Z_0 = 75.1\%$) and three-phase power loss ($P_0 = 71.9$ kW) measured in the test HOO at $V_0 = 7.7\%$ (these P_0 and Z_0 are represented by points 4 in Figs. 2 and 16, respectively).

Although the solid lines in Fig. 16 obviously deviate from the dashed Z_0 curves calculated with the lumped-distributed models 1 - 4, it is remarkable that model [10] reproduces accurately power losses P_0 for all the voltages V_0 and tests listed in Table 1. (The calculated P_0 curves are close to those shown in Fig. 2).

In connection with modeling ZS losses above and due to the fact that losses P_0 are often not measured in ZS tests,

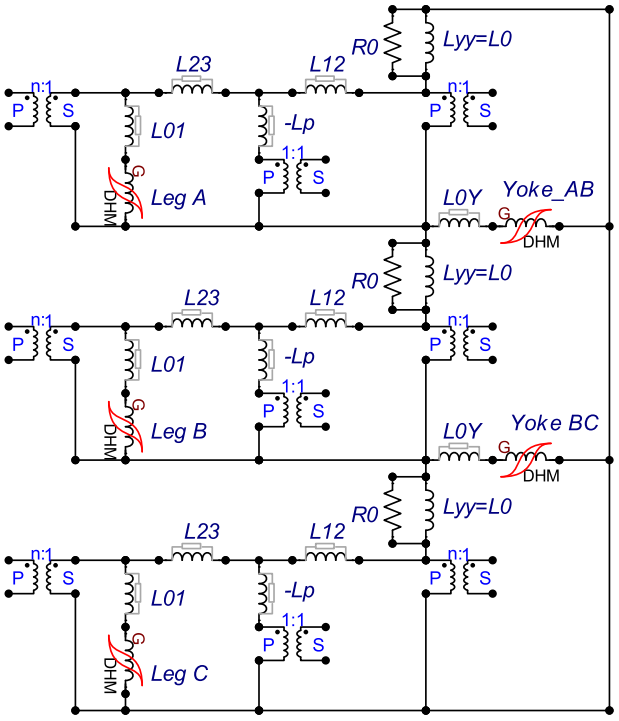

FIGURE 15. Lumped parameters model [10] extended to three-winding transformer.

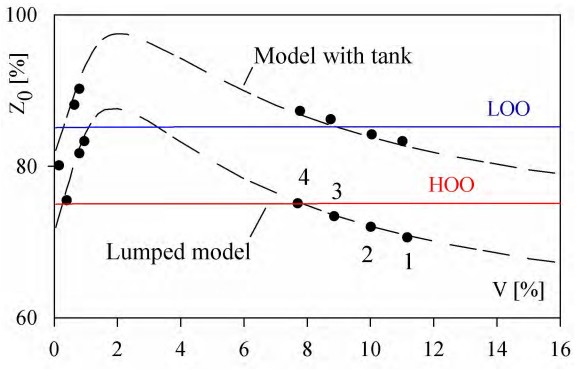

FIGURE 16. ZS impedances calculated with model [10] fitted to point 4.

it was also interesting to simplify the L_0R_0 model [10] by omitting resistances R_0. (This model will be referred to as the L_0 model). To keep the same ZS impedance, inductance L_0 of such a model should be taken approximately 6% less than that in the original L_0R_0 model. A detail comparison of L_0 and L_0R_0 models has not revealed any visible difference in their SC and inrush currents for YNyn, YNynd, and Yynd winding connections. The difference of 5% was found only for Yyn transformer.

A maximum difference of 12% was found between inrush current results predicted by models L_0R_0 and L_0, on the one hand, and corresponding currents in Table 3 calculated with the lumped-distributed models 1 - 4. An even smaller, three percent difference between current peaks predicted by these models was observed on a 300 kVA Yyn distribution transformer studied experimentally in [22] and modeled in [20].

Similar maximum difference (9%) was found in SC currents. Taking into account associated uncertainties in the network parameters, these differences should be considered acceptable in these regimes.

The large difference between the reactive power Q predicted by model [10] and models 1 – 4 (see Table 4) can be explained by the fact that in the lumped parameter model [10], there is no subdivision of the ZS flux between the flux returning through the tank and the one closing in air/oil. Besides, in contrast to models 1 to 4, no parameters of the tank wall (its thickness, height, material properties) is used in model [10]. As a result, the maximum flux density in the legs (B_m), reached at GIC condition, is lower than that predicted with models 1 – 4.

As can be seen in Table 4, there is a correlation between B_m and the value of Q. Whereas the value of B_m reached in this 3L transformer does not exceed 2.044 T, its value in the equivalent 5L transformer reaches 2.111 T at the same GIC. In the oversaturated region, this difference is very large and determines the difference between 3L and 5L transformers under GIC conditions.

VII. CONCLUDING REMARKS

We have studied transient topological models of a three-legged core type transformer, which take into account the tank walls considered as a distributed parameter structure. Processes in the walls are described by Cauer circuits (hysteretic and anhysteretic), which represent a tank wall belt (TWB) that is a zone of maximum circumferential eddy-currents encircling simultaneously all three wound legs. The latter distinguishes the models developed from other simulation tools, in which each core leg has individual fictitious tank with no possibility of studying processes in the tank wall depth.

Model 1 studied in the paper is that in [5], in which the height of the TWB was taken equal to the height of the core window or 60% of the tank wall height. Although this model replicates accurately all possible zero-sequence (ZS) impedances of the three-winding transformer, it was found that it yields about 2/3 of the power loss P_0 measured in the ZS tests HOO and LOO specified in Table 1.

It is remarkable that almost the same underestimate in P_0 was observed in model 2, in which the TWB height was increased to 95% of the tank height.

To explore whether it is necessary to reproduce accurately the ZS loss P_0 obtained in the measurement of ZS *magnetizing* impedances, i.e. in the HOO and LOO tests, we have improved the models 1 and 2 by introducing eddy-current resistors R_{loss} into each of them. The thus obtained models 3 and 4 have eliminated the 30-35 percent underestimates of the ZS loss P_0, while keeping the accuracy in ZS impedances.

It was shown that the introduction of R_{loss} does not lead to noticeable changes in the model behavior during inrush and

short circuit events, but requires an increase in inductance L_T of the models (see Table 2) that changes the model behavior under GIC. On the other hand, as could be expected from almost dc flux in the tank under a large GIC, the presence of the eddy-current R_{loss} has *no effect* on modeling GIC influence. So, resistor R_{loss} can be omitted under GIC conditions in models 3 and 4 while keeping remaining model parameters. This leads to the conclusion that models 1 and 2, which have no R_{loss}, may be used irrespective of the transformer operation, despite their underestimate of ZS losses P_0.

Similar to current peaks, the absence of R_{loss} and hence understated ZS losses shown by models 1 and 2 have no noticeable influence on the decay of the inrush current when comparing these models with models 3 and 4 and with the conventional lumped parameters model in [10]. The latter can be used in its original L_0R_0 form or in the form with only inductances L_0 employed in many models.

The only marked difference between the models 1 to 4 and model in [10] was found in modeling GIC influence. The reason is that no tank parameters can be accounted in [10]. On the contrary, the height of the TWB can be used as a fitting parameter in the models 1 to 4 in the presence of GIC.

To pre-empt possible questions about finding R_{loss} from Maxwell equations, it should be emphasized that the models considered are essentially circuital. So the detailed evaluation of R_{loss} as well as resistors R_0 in [10] (see Fig. 15 above) is hardly possible within any circuital modeling. These elements can only be found using the measured data. On the other hand, we have shown a negligible role of R_{loss} and R_0 in modeling inrush currents and short circuit faults. The evaluation of the models under GIC conditions requires reliable experimental data.

Therefore, it can be concluded that the models proposed in the paper are topological models that reproduce accurately transformer behavior under both positive- and zero-sequence excitations. They can be used to explain transformer operation details under abnormal conditions and evaluate applicability of simplified low-frequency transformer models.

REFERENCES

[1] F. de León, P. Gómez, J. A. Martinez-Velasco, and M. Rioual, "Transformers," in *Power System Transients: Parameter determination*, J. A. Martinez-Velasco, Ed. Boca Raton, FL, USA: CRC Press, 2009, pp. 177–249.

[2] S. Jazebi, S. E. Zirka, M. Lambert, A. Rezaei-Zare, N. Chiesa, Y. Moroz, X. Chen, M. Martinez-Duro, C. M. Arturi, E. P. Dick, A. Narang, R. A. Walling, J. Mahseredjian, J. A. Martinez, and F. de León, "Duality derived transformer models for low-frequency electromagnetic transients—Part I: Topological models," *IEEE Trans. Power Del.*, vol. 31, no. 5, pp. 2410–2419, Oct. 2016.

[3] S. Jazebi, A. Rezaei-Zare, M. Lambert, S. E. Zirka, N. Chiesa, Y. I. Moroz, X. Chen, M. Martinez-Duro, C. M. Arturi, E. P. Dick, A. Narang, R. A. Walling, J. Mahseredjian, J. A. Martinez, and F. de León, "Duality-derived transformer models for low-frequency electromagnetic transients—Part II: Complementary modeling guidelines," *IEEE Trans Power Del.*, vol. 31, no. 5, pp. 2420–2430, Oct. 2016.

[4] *Literature Survey on Transformer Models for the Simulation of Electromagnetic Transients With Emphasis on Geomagnetic-Inducted Current (GIC) Applications*. EPRI, Palo Alto, CA, USA, 2012, Art. no. 1025844.

[5] S. E. Zirka, Y. I. Moroz, and C. M. Arturi, "Accounting for the influence of the tank walls in the zero-sequence topological model of a three-phase, three-limb transformer," *IEEE Trans. Power Del.*, vol. 29, no. 5, pp. 2172–2179, Oct. 2014.

[6] S. E. Zirka, Y. I. Moroz, and E. Rahimpour, "Towards a transformer transient model as a lumped-distributed parameter system," *COMPEL-Int. J. Comput. Math. Elect. Electron. Eng.*, vol. 36, no. 3, pp. 741–750, Jan. 2017.

[7] A. Ramos, J. C. Burgos, A. Moreno, and E. Sorrentino, "Determination of parameters of zero-sequence equivalent circuits for three-phase three-legged YNynd transformers based on onsite low-voltage tests," *IEEE Trans. Power Del.*, vol. 28, no. 3, pp. 1618–1625, Jul. 2013.

[8] E. Sorrentino and J. C. Burgos, "Application of 2D linear models for computing zero-sequence magnetizing impedances of 3-phase core-type transformers," *Electr. Power Syst. Res.*, vol. 117, pp. 123–133, Dec. 2014.

[9] Sorrentino, J. C. Burgos, "Application of 2D linear modeling for computing zero-sequence short-circuit impedances of 3-phase core-type YNynd transformers," *Electr. Power Syst. Res.*, vol. 122, pp. 1–9, 2015.

[10] J. A. Martínez, R. Walling, B. A. Mork, J. Martin-Arnedo, and D. Durbak, "Parameter determination for modeling system transients—Part III: Transformers," *IEEE Trans. Power Del.*, vol. 20, no. 3, pp. 2051–2062, Jul. 2005.

[11] O. Biro, G. Koczka, G. Leber, K. Preis, and B. Wagner, "Finite element analysis of three-phase three-limb power transformers under DC bias," *IEEE Trans. Magn.*, vol. 50, no. 2, Feb. 2014, Art. no. 7013904.

[12] J. Winders, *Power Transformers: Principles and Applications*. New York, NY, USA: Marcel Dekker, 2002.

[13] S. V. Kulkarni and S. A. Khaparde, *Transformer Engineering: Design and Practice*. New York, NY, USA: Marcel Dekker, 2004.

[14] S. E. Zirka, Y. I. Moroz, N. Chiesa, R. G. Harrison, and H. K. Høidalen, "Implementation of inverse hysteresis model into EMTP—Part II: Dynamic model," *IEEE Trans. Power Del.*, vol. 30, no. 5, pp. 2233–2241, Oct. 2015.

[15] Y. I. Moroz and S. E. Zirka. (Apr. 9, 2019). *Inverse Models of Magnetic Hysteresis*. [Online]. Available: https://sites.google.com/site/inverse-hysteresismodel

[16] S. E. Zirka, Y. I. Moroz, N. Chiesa, R. G. Harrison, and H. K. Høidalen, "Implementation of inverse hysteresis model into EMTP—Part I: Static model," *IEEE Trans. Power Del.*, vol. 30, no. 5, pp. 2224–2232, Oct. 2015.

[17] A. Lotfi, H. Kr Høidalen, E. Agheb, and A. Nysveen, "Characterization of magnetic losses in the transformer tank steel," *IEEE Trans. Magn.*, vol. 52, no. 5, May 2016, Art. no. 6301104.

[18] N. Tleis, *Power Systems Modelling and Fault Analysis: Theory and Practice*. New York, NY, USA: Elsevier, 2008.

[19] R. M. Del Vecchio, B. Poulin, P. T. Feghali, D. M. Shah, and R. Ahuja, *Transformer Design Principles: With Applications to Core-Form Power Transformers*, 2nd ed. New York, NY, USA: CRC Press, 2010.

[20] S. E. Zirka, Y. I. Moroz, H. K. Høidalen, A. Lotfi, N. Chiesa, and C. M. Arturi, "Practical experience in using a topological model of a core-type three-phase transformer—No-load and inrush conditions," *IEEE Trans. Power Del.*, vol. 32, no. 4, pp. 2081–2090, Aug. 2017.

[21] R. A. Walling and A. H. Khan, "Characteristics of transformer exciting-current during geomagnetic disturbances," *IEEE Trans. Power Del.*, vol. 6, no. 4, pp. 1707–1714, Oct. 1991.

[22] N. Chiesa, B. A. Mork, and H. K. Høidalen, "Transformer model for inrush current calculations: Simulations, measurements and sensitivity analysis," *IEEE Trans. Power Del.*, vol. 25, no. 4, pp. 2599–2608, Oct. 2010.

JIANHUI ZHAO received the Ph.D. degree from the Department of Power Machinery, Bauman Moscow State Technical University, in 2013. He was as an Associate Professor with Harbin Engineering University, China, in October 2013, and engaged in the design and research of electromagnetic actuators for diesel engines, where he became a Professor, in 2018, researching the simulation of dynamic hysteretic characteristics of high-speed electromagnetic actuators and the development of fuel system for marine diesel engine.

SERGEY E. ZIRKA received the Ph.D. and D.Sc. degrees in electrical engineering from the Institute of Electrodynamics, Kiev, Ukraine, in 1977 and 1992, respectively. Since 1972, he has been with Dnepropetrovsk (currently Dnipro) National University, Ukraine, where he has been a Professor, since 1992. His research interests include the modeling of magnetization processes in electrical steels, forming and transforming high-energy pulses, and transients in transformers of different types.

YURIY I. MOROZ received the Ph.D. degree in theoretical electrical engineering from the Institute of Modeling Problems in Energetics, Ukrainian Academy of Sciences, Kiev, Ukraine, in 1991.

He is currently an Associate Professor with the Department of Physics and Technology, Dnipro National University, Ukraine. His research interests include modeling of magnetization processes in electrical steels and transients in transformers of different types.

CESARE M. ARTURI (M'87) received the electrical engineering degree from the Politecnico di Milano, Milan, Italy, in 1975.

He is currently a Full Professor with the Department of Electronics, Information and Bioengineering (DEIB), Politecnico di Milano. His research interests include the modeling of parametric energy conversion devices, power transformers, and the thermodynamic approach to the electromagnetic conversion devices.

REIGH A. WALLING received the B.S. and M.Eng. in electric power engineering from the Rensselaer Polytechnic Institute, in 1974 and 1979, respectively.

He was with the GE's Energy Consulting Business Group for 32 years. Prior to GE, he was with Minnesota Power. He is currently the President and Principal of Walling Energy Systems Consulting, LLC, where he is engaged in a diverse range of transmission, distribution, renewable energy, and distributed generation technologies and issues, serving electric utility, Government power plant developer, and research institution clients. He is also a Licensed Professional Engineer in Minnesota. He has authored over 95 papers and articles, and he holds 20 patents. He was a recipient of the IEEE Power and Energy Society Power Distribution Award, in 2009.

NASSER TLEIS received the M.Sc. and Ph.D. degrees in electric power engineering from the University of Manchester Institute of Science and Technology (UMIST), U.K, in 1986 and 1989, respectively.

He is currently the Vice President of power transmission planning with Dubai Electricity and Water Authority (DEWA), where he is engaged in a diverse range of generation and transmission planning, demand forecasting, renewable energy integration, generation and power plant technologies, advanced power plant and system modeling, and analysis and studies. Prior to joining DEWA, in 2010, he worked for 26 years in the U.K.'s electricity supply industry for the CEGB and then, the National Grid Company PLC. He is a Chartered Engineer registered with the Engineering Council, U.K. He has authored over 25 papers and 2 books. He is a Fellow of the IET (formerly IEE) and also a member of CIGRE. He was awarded the IEE Electric Power Applications John Hopkinson's Premium, in 1990.

OLEXANDR L. TARCHUTKIN received the electrical engineering degree from the Zaporizhzhya National Technical University, Ukraine, in 1994.

He was the Project Manager of transformer design up to 750 kV in the Ukraine Office, Soft Team Group, from June 2010 to June 2016—TEO in the Global PT Corporation (GPT), Los Angeles, USA. From 1998 to 2010, he was the Chief of the Laboratory in the JSC ''VIT'' Ukrainian Research, Design and Technological Transformer Institute, Zaporizhzhya, Ukraine. Since 2017, he has been a Team Leader of the Soft Team Group. He has also been the Project Manager of transformer and reactor design up to 1100kV, HVDC transformer up to $\pm$800 kV and software developing.